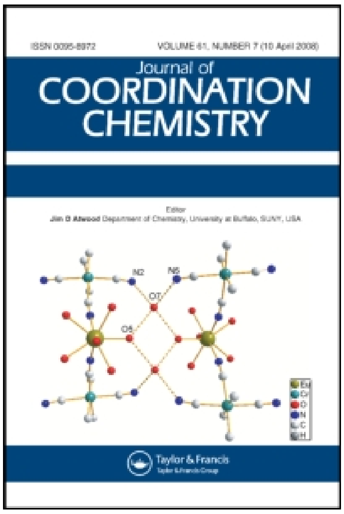

Journal of Coordination Chemistry
Publication details, including instructions for authors and subscription information:
http://www.informaworld.com/smpp/title~content=t713455674

Supramolecular complexes constructed with carboxylate Cu(II) and 2-(2-pyridyl)-benzimidazole via hydrogen bonding

Li-Jun Zhou[a]; Xin-Jun Luan[a]; Yao-Yu Wang[a]; Gene-Hsiang Lee[b]; Qi-Zhen Shi[a]; Shie-Ming Peng[b]
[a] Department of Chemistry & Shaanxi Key Laboratory of Physico-Inorganic Chemistry, Northwest University, Xi'an 710069, Shaanxi, P.R. China [b] Department of Chemistry, National Taiwan University, Taiwan

To cite this Article Zhou, Li-Jun , Luan, Xin-Jun , Wang, Yao-Yu , Lee, Gene-Hsiang , Shi, Qi-Zhen and Peng, Shie-Ming(2006) 'Supramolecular complexes constructed with carboxylate Cu(II) and 2-(2-pyridyl)-benzimidazole via hydrogen bonding', Journal of Coordination Chemistry, 59: 10, 1107 — 1121

To link to this Article: DOI: 10.1080/00958970500425962

URL: http://dx.doi.org/10.1080/00958970500425962

Journal of Coordination Chemistry
Vol. 59, No. 10, 10 July 2006, 1107–1121

Taylor & Francis
Taylor & Francis Group

Supramolecular complexes constructed with carboxylate Cu(II) and 2-(2-pyridyl)-benzimidazole via hydrogen bonding

LI-JUN ZHOU†, XIN-JUN LUAN†, YAO-YU WANG*†,
GENE-HSIANG LEE‡, QI-ZHEN SHI† and SHIE-MING PENG‡

†Department of Chemistry & Shaanxi Key Laboratory of Physico-Inorganic Chemistry,
Northwest University, Xi'an 710069, Shaanxi, P.R. China
†Department of Chemistry, National Taiwan University, Taiwan

(*Received 13 June 2005; in final form 22 July 2005*)

Four copper(II) supramolecular complexes, $\{[Cu(Hpb)(mal)]\cdot H_2O\}_n$ (**1**), (Hpb = 2-(2-pyridyl)-benzimidazole, mal = maleate), $[Cu_4(pb)_4(cro)_4(MeOH)_2]\cdot 2MeOH$ (**2**) (cro = crotonate), $[Cu_2(pb)(Hpb)(mac)_3(MeOH)]$ (**3**) (mac = α-methacrylate) and $[Cu(Hpb)(acr)_2(H_2O)]$ (**4**) (acr = acrylate), based on carboxylate copper(II)-aromatic ligand systems which are assembled by combination of metal coordination, hydrogen-bond and π–π interactions, have been rationally designed and synthesized. Complex **1** forms a 3D supramolecular network with open channels by extending 2D undulating sheets constructed from 1D helical chains. Complex **2** generates a 2D grid-like sheet *via* unusual finite-chain tetranuclear molecules, with four copper atoms arranged in a line; the unit does not extend further due to the capping effect of the terminal methanol. Complexes **3** and **4** present a 1D sinusoidal structure and a 3D columnar network with 1D ladder-shaped double chains, respectively. Interestingly, coligand Hpb, deprotonated or/and neutral in different supramolecular complexes, provides hydrogen bonding and π–π stacking interactions. In complexes **2**, **3** and **4**, carboxylate anions show various bridging modes, which are reflected in their magnetic properties. Weak ferromagnetic coupling (syn-anti μ-OCO) exists in **1**, antiferromagnetic (syn-syn μ-OCO) and weak ferromagnetic coupling (μ-O of the −COO group) in **2** and antiferromagnetic coupling (syn-syn μ-OCO) in **3**.

Keywords: Supramolecular complexes; Carboxylate Cu(II); 2-(2-Pyridyl)-benzimidazole; Magnetic properties

1. Introduction

With the rapid development of supramolecuar chemistry of metal complexes, a large number of supramolecular coordination compounds have been constructed

---

*Corresponding author. Tel.: +862988303097. Fax: +86 29 88373398. Email: wyaoyu@nwu.edu.cn

Journal of Coordination Chemistry
ISSN 0095-8972 print: ISSN 1029-0389 online © 2006 Taylor & Francis
DOI: 10.1080/00958970500425962

by coordination molecules which consist of metal ions (and metal clusters) functioning as nodes and organic ligands as bridges, through coordination bonding, hydrogen bonding, π–π stacking interactions as well as van der Waals forces [1–3] and exhibit a wide range of infinite 0D, 1D, 2D or 3D frameworks with different interesting structural features [4, 5]. On the other hand, many coordination supramolecular structures based on metal-organic ligands, in fact, have been designed for purely symmetry and esthetic grounds. The intense interest in this field, given impetus by synthetic and theoretical chemists, crystallographers and materials scientists, has resulted not only in beautiful and diversified structures, but also in potential applications as electronic, magnetic, optical, absorbent and catalytic materials [6]. However, recognition and assembly of supramolecules is intricate because the factors influencing the formation of the ultimate structures are various. Rational design and synthesis of multifunctional compounds and materials with predictable structures and properties is still one of the most challenging research fields in modern chemistry. Many investigations indicate that the proper choice of ligand as well as metal ion is very important for designing the target metal-ligand coordination supramolecular complexes [7] with different structural features and potential functions.

Planar chelated coligand 2-(2-pyridyl)-benzimidazole is good not only because it can bond metal ions through coordination bonding interactions but also because it can supply hydrogen-bonding interactions as hydrogen donor or acceptor through active imidazole hydrogen [8] (–NH–) and can also offer π–π stacking interactions to form multi-dimensional supramolecular networks. Besides the terminal planar ligands, bridging ligands are also very important. Among the bridging ligands that originate low-dimensional complexes, carboxylate is one of the most widely used for designing supramolecular complexes [9–11]. Its versatility as ligand is illustrated by the variety of its coordination modes, such as "free", monodentate, chelating and bridging.

In our recent work on supramolecular assembly of carboxylates, we have fabricated structures of oligonuclear species, one-, two-, and three-dimensional systems with novel structural properties [12]. As an extension of our studies on carboxylate copper(II) complexes, in this article, we use 2-(2-pyridyl)-benzimidazole (Hpb) as terminal ligand and different carboxylates as bridging ligands to synthesize four novel complexes, where the carboxylate groups exhibit a wide variety of binding modes. Complex **1**, $\{[Cu(Hpb)(mal)]\cdot H_2O\}_n$ is a 1D helical chain polymer producing a 3D network with open channels. Complex **2**, $[Cu_4(pb)_4(cro)_4(MeOH)_2]\cdot 2MeOH$, shows a linear tetranuclear structure where four copper atoms are bridged by four crotonates. From our previous investigation, it is unusual for monocarboxylate to form finite-chain multinuclear structures. The tetranulear units extend into a 2D sheet with solvent molecules located in the grids. Complex **3**, $[Cu_2(pb)(Hpb)(mac)_3(MeOH)]$ and complex **4**, $[Cu(Hpb)(acr)_2(H_2O)]$ have a dinuclear and a monomolecular structure, respectively. Moreover, **3** and **4** generate a 1D sinusoidal chain and a 3D supramolecular network, respectively, through hydrogen bonding and π–π stacking interactions. Complexes **1**, **2** and **3** have different bridging modes of carboxylate anions, which are reflected in their magnetic properties. Complex **1** shows weak ferromagnetic coupling. There is a weak ferromagnetic interaction in complex **2**, but the global interaction is antiferromagnetic. Complex **3** shows strong antiferromagnetic coupling.

2. Experimental

2.1. *Physical measurements*

Elemental analyses were determined with a Perkin-Elmer model 240C instrument. Infrared spectra (KBr) pellets were recorded on a Nicolet 170SX FT-IR spectrophotometer in the range 4000–400 cm^{-1}. TGA analyses were recorded with a NETZSCH STA 449C microanalyzer in an atmosphere of nitrogen at a heating rate of 5°C min^{-1}. Variable-temperature magnetic susceptibility measurements were carried out on an Oxford Maglab 2000 magnetometer with an applied field of 20000 G. Diamagnetic correction was estimated from Pascal's constants.

2.2. *Materials*

Hpb was purchased from Aldrich Company. $Cu(mal) \cdot H_2O$, $Cu_2(CH_3CH{=}CHCO_2)_4(H_2O)_2$, $Cu_2[CH_2{=}C(CH_3)CO_2]_4(H_2O)_2$ and $Cu_2(CH_2{=}CHCO_2)_4(H_2O)_2$ were prepared according to the literature [13]. All other reagents were commercially available and used without further purification.

2.3. *Preparations*

2.3.1. $\{[Cu(Hpb)(mal)] \cdot H_2O\}_n$ (1). An H tube was filled with methanol solution (10 mL) of Hpb (0.1953 g, 1 mmol) in one side and maleate copper(II) (0.1955 g, 1 mmol) aqueous solution (10 mL) in the other allowing very careful diffusion. Several days later, diamond sky-blue crystals of **1** were obtained at the middle silver sand with the yield of 46%. Anal. Calcd for $C_{16}H_{13}N_3O_5Cu$: C, 49.17; H, 3.35; N, 10.75. Found: C, 50.09; H, 3.37; N, 10.83%. IR (KBr): $\nu = 3447$, 2920, 1642, 1568, 1398, 1153, 1050, 801, 755 cm^{-1}.

2.3.2. $[Cu_4(pb)_4(cro)_4(MeOH)_2] \cdot 2MeOH$ (2). A solution of crotonate copper(II) (0.2522 g, 0.5 mmol) in 10 mL methanol was layered upon a $CHCl_3$ solution (5 mL) of Hpb (0.1953 g, 1 mmol) in a sealed tube with very careful diffusion. After several days, rectangle green crystals of **2** were obtained with yield of 65%. Anal. Calcd for $C_{68}H_{68}N_{12}O_{12}Cu_4$: C, 54.47; H, 4.57; N, 11.21. Found: C, 54.59; H, 4.62; N, 11.17%. IR (KBr): $\nu = 3415$, 3055, 1657, 1562, 1391, 1280, 969, 741 cm^{-1}.

2.3.3. $[Cu_2(pb)(Hpb)(mac)_3(MeOH)]$ (3). A methanol solution (5 mL) of Hpb (0.1953 g, 1 mmol) was added to a solution of α-methacrylate copper(II) (0.2519 g, 0.5 mmol) in 10 mL methanol. The mixture was stirred for 15 min and then filtered. The resulting solution was diffused in diethyl ether at room temperature for two weeks, and triangle greenblue crystals of **3** were obtained in 52% yield. Anal. Calcd for $C_{37}H_{36}N_6O_7Cu_2$: C, 55.29; H, 4.51; N, 10.46. Found: C, 54.99; H, 4.46; N, 10.37%. IR (KBr): $\nu = 3398$, 3059, 1658, 1578, 1334, 1283, 958, 728 cm^{-1}.

2.3.4. $[Cu(Hpb)(acr)_2(H_2O)]$ (4). A methanol solution (5 mL) of Hpb (0.1953 g, 1 mmol) was added to a solution of acrylate copper(II) (0.2222 g, 0.5 mmol) in 15 mL of methanol/water. The mixture was stirred for 20 min and then filtered. The resulting solution was diffused in diethyl ether at room temperature for several days, and quadrangle green crystals of **4** were obtained in 77% yield. Anal. Calcd for $C_{18}H_{17}N_3O_5Cu$: C, 51.61; H, 4.09; N, 10.03. Found: C, 51.59; H, 4.13; N, 10.13%. IR (KBr): $\nu = 3445, 3082, 1627, 1563, 1380, 1285, 952, 730\,cm^{-1}$.

2.4. *X-ray crystallography*

X-ray diffraction data were collected with graphite monochromated Mo-Kα radiation ($k = 0.71073$ Å) on a NONIUS Kappa CCD diffractometer for complex **1** at 150(1) K and on a BRUKER SMART APEXCCD diffractometer for complexes **2**, **3** and **4** at 273(2) K. The structures were solved by direct methods [14] and refined by full-matrix least-squares on F^2 with the SHELXL-97 program package [15]. The non-hydrogen atoms were located with difference Fourier synthesis, and the hydrogen atoms were generated geometrically. The crystallographic data for **1**–**4** are listed in table 1, and selected bond lengths and angles for **1**–**4** are presented in table 2.

3. Results and discussion

3.1. *Crystal structures*

A single-crystal X-ray structural analysis shows that **1** consists of one copper(II) ion, one Hpb, two maleate and one lattice water molecule in each independent crystallographic unit. Each copper atom is coordinated by three oxygen atoms from two maleate ligands (Cu1–O1 2.224(2), Cu1–O2A 1.935(2) and Cu1–O3A 1.966(3) Å) and two nitrogen atoms from a chelating Hpb ligand (Cu1–N1 2.045(3) and

Table 1. Crystallographic data and structure refinement summary for complexes **1**–**4**.

	1	**2**	**3**	**4**
Empirical formula	$C_{16}H_{13}N_3O_5Cu$	$C_{68}H_{68}N_{12}O_{12}Cu_4$	$C_{37}H_{36}N_6O_7Cu_2$	$C_{18}H_{17}N_3O_5Cu$
Formula mass	390.83	1499.50	806.80	418.89
Temperature (K)	150(1)	273(2)	273(2)	273(2)
Crystal system	Monoclinic	Triclinic	Triclinic	Monoclinic
Space group	$P2_1/n$	P-1	P-1	$P2_1/c$
a (Å)	12.520(2)	10.129(2)	12.423(3)	6.909(2)
b (Å)	6.724(1)	12.195(3)	12.653(3)	18.281(6)
c (Å)	18.836(3)	14.697(3)	12.875(3)	15.007(5)
α (°)	90.000	81.992(3)	67.772(4)	90.000
β (°)	108.694(5)	81.701(3)	84.512(4)	98.156(6)
γ (°)	90.000	66.085(3)	83.636(4)	90.000
V (Å^3), Z	1502.0(4), 4	1635.5(6), 1	1858.7(7), 4	1876.3(10), 4
D_{calcd} (g cm^{-3})	1.728	1.516	1.436	1.483
μ (mm^{-1})	1.490	1.355	1.200	1.198
F(000)	796	766	828	860
Limiting indices	$-16 \le h \le 16$, $-8 \le k \le 8$, $-24 \le l \le 24$	$-13 \le h \le 13$, $-15 \le k \le 16$, $-16 \le l \le 19$	$-10 \le h \le 13$, $-13 \le k \le 13$, $-13 \le l \le 12$	$-8 \le h \le 8$, $-20 \le k \le 22$, $-18 \le l \le 15$
Data/restraints/parameters	3443/0/227	7599/1/457	4912/2/479	3426/0/250
R(int)	0.0392	0.0277	0.0388	0.0408
Goodness-of-fit	1.197	0.940	0.990	1.059
R_1, wR_2 [$I > 2\sigma(I)$]	0.0501, 0.1408	0.0481, 0.1239	0.0648, 0.1664	0.0534, 0.1445
R_1, wR_2 (all data)	0.0678, 0.1605	0.0722, 0.1349	0.1117, 0.1922	0.0962, 0.1646

Table 2. Selected bond lengths (Å) and bond angles (°) for complexes **1**–**4**.

*Complex **1***			
Cu(1)–O(2A)	1.935(2)	Cu(1)–O(3A)	1.966(3)
Cu(1)–N(2)	1.986(3)	Cu(1)–N(1)	2.045(3)
Cu(1)–O(1)	2.224(2)		
O(2A)–Cu(1)–O(3A)	91.82(2)	O(3A)–Cu(1)–N(2)	94.85(2)
O(2A)–Cu(1)–N(1)	92.70(2)	N(2)–Cu(1)–N(1)	81.16(2)
O(2A)–Cu(1)–O(1)	83.51(2)	O(3A)–Cu(1)–O(1)	112.24(2)
N(2)–Cu(1)–O(1)	93.96(2)	N(1)–Cu(1)–O(1)	90.99(2)
*Complex **2***			
Cu(1)–N(2)	1.941(2)	Cu(1)–N(1)	2.028(2)
Cu(1)–O(1)	1.951(2)	Cu(1)–O(3)	1.9718(2)
Cu(1)–O(3A)	2.414(2)	Cu(2)–N(4)	2.040(3)
Cu(2)–N(5)	1.931(2)	Cu(2)–O(2)	1.943(2)
Cu(2)–O(4)	1.981(2)	Cu(2)–O(5)	2.249(2)
N(2)–Cu(1)–O(1)	93.06(9)	O(1)–Cu(1)–O(3)	91.24(8)
N(2)–Cu(1)–N(1)	81.78(2)	O(3)–Cu(1)–N(1)	92.97(9)
N(2)–Cu(1)–O(3A)	111.82(9)	O(1)–Cu(1)–O(3A)	88.37(8)
O(3)–Cu(1)–O(3A)	75.96(8)	N(1)–Cu(1)–O(3A)	100.14(8)
N(5)–Cu(2)–O(4)	94.53(2)	O(2)–Cu(2)–O(4)	91.21(9)
N(5)–Cu(2)–N(4)	81.91(2)	O(2)–Cu(2)–N(4)	91.53(2)
N(5)–Cu(2)–O(5)	96.72(2)	O(2)–Cu(2)–O(5)	89.87(9)
O(4)–Cu(2)–O(5)	95.16(9)	N(4)–Cu(2)–O(5)	91.88(9)
*Complex **3***			
Cu(1)–O(1)	1.943(5)	Cu(1)–O(3)	1.953(5)
Cu(1)–N(1)	1.952(6)	Cu(1)–N(3)	2.027(6)
Cu(1)–O(5)	2.290(6)	Cu(2)–O(2)	1.938(5)
Cu(2)–O(4)	1.962(5)	Cu(2)–N(4)	1.963(7)
Cu(2)–N(6)	2.067(7)	Cu(2)–O(6)	2.179(6)
O(1)–Cu(1)–N(1)	95.9(2)	O(1)–Cu(1)–O(3)	89.5(2)
N(1)–Cu(1)–N(3)	81.5(3)	O(3)–Cu(1)–N(3)	92.1(2)
O(1)–Cu(1)–O(5)	94.9(2)	N(1)–Cu(1)–O(5)	94.7(2)
O(3)–Cu(1)–O(5)	94.2(2)	N(3)–Cu(1)–O(5)	91.6(2)
O(2)–Cu(2)–O(4)	91.5(2)	O(4)–Cu(2)–N(4)	96.1(3)
O(2)–Cu(2)–N(6)	89.5(3)	N(4)–Cu(2)–N(6)	81.1(3)
O(2)–Cu(2)–O(6)	95.3(2)	O(4)–Cu(2)–O(6)	93.1(2)
N(4)–Cu(2)–O(6)	97.1(2)	N(6)–Cu(2)–O(6)	95.4(2)
*Complex **4***			
Cu(1)–O(3)	1.925(4)	Cu(1)–O(1)	1.984(4)
Cu(1)–N(2)	1.990(4)	Cu(1)–N(1)	2.054(4)
Cu(1)–O(5)	2.248(4)		
O(3)–Cu(1)–O(1)	91.62(2)	O(1)–Cu(1)–N(2)	93.37(2)
N(2)–Cu(1)–N(1)	80.56(2)	O(3)–Cu(1)–N(1)	91.16(2)
O(3)–Cu(1)–O(5)	93.38(2)	O(1)–Cu(1)–O(5)	101.42(2)
N(2)–Cu(1)–O(5)	97.35(2)	N(1)–Cu(1)–O(5)	95.78(2)

Cu1–N2 1.986(3) Å) in a distorted square-pyramidal geometry (figure 1a) with deviation of Cu1 away from the equatorial plane (N1, N2, O2, O3) by 0.2070 Å towards O1. In this complex, maleate not only chelated end to end to one copper(II) atom forming a heptagonal ring but also bridged to an adjacent unit. As a result, a neutral 1D helical chain is fabricated in which equivalent atoms are related by a 2_1-screw axis along the *b*-axis (figure 1b), with carboxylate groups from one maleate occupying the basal position (O2, O3) in the former unit and the apical position (O1) in the latter unit. The pitch of the helix is 6.724 Å and the shortest Cu $\cdots$ Cu intrachain separation is 5.396 Å, shorter than the distance (6.541 Å) in the complex $[Cd_2(mal)_3(H_2O)_6]$

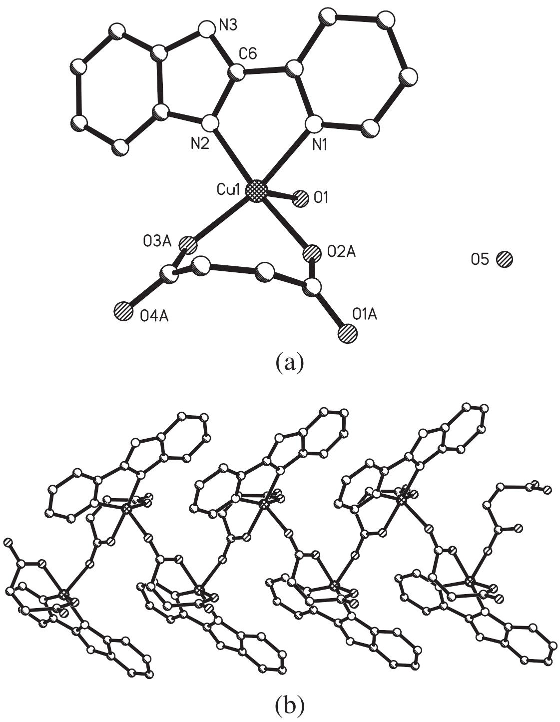

Figure 1. (a) The coordination environment of Cu ion in **1**, hydrogen atoms omitted for clarity. (b) The 1D helical chain. (c) The 2D undulating network. Hpb omitted for clarity. (d) The 3D network structure.

(H_2mal = malonic acid) [16] in which the carboxylate groups have similar coordination modes. In fact, the distance produced by this bridging is shorter than that by dimonodentate, dichelate or monodentate-chelate carboxylate bridging [17]. The chiral chain has Hpb ligands in two different orientations alternately attached to both sides of the helix with a dihedral angle of 66.00°. There also exist aromatic π–π stacking interactions of Hpb in the chain. It should be noted that the lattice water molecules play key roles in the polymer. Each two water molecules quadruple-hydrogen bond to adjacent helical chains resulting in an undulating 2D supramolecular network with helical chains arranged in an $\cdots$ABAB$\cdots$ fashion as shown in figure 1(c). The 2D layers extend into a 3D network with open channels *via* N3–H3A$\cdots$O4 (2.790 Å, 173.60°) hydrogen bonding interactions between 2D networks (figure 1d).

When crotonate of a monocarboxylate was used instead of maleate, it led to a novel linear tetranuclear copper(II) compound **2** which consists of doubly-bridged dimeric copper(II) units arranged around a centre of symmetry and linked by an oxygen atom of crotonate that acts as a bridging donor (figure 2a). The coordination environment around each copper atom is approximately square pyramidal with two nitrogen donors of deprotonated chelating Hpb and two oxygen atoms from two crotonate occupying the basal sites (average Cu–N 1.985, Cu–O 1.962 Å). A bridging oxygen O3 and a methanol are located at the apical positions at slightly longer distances (average Cu–O 2.332 Å). In each dimeric unit two copper atoms are separated by 2.989(3) Å and the deviation of Cu1 and Cu2 away from the corresponding equatorial plane is 0.1439 and 0.1368 Å toward O3A and O5, respectively. The two antiparallel

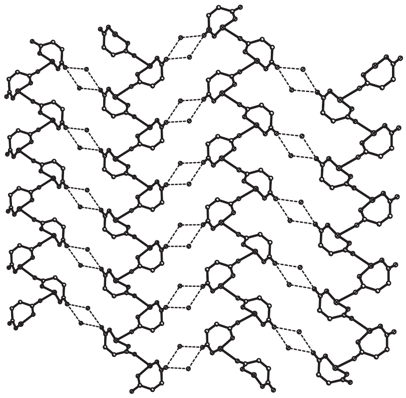

(c)

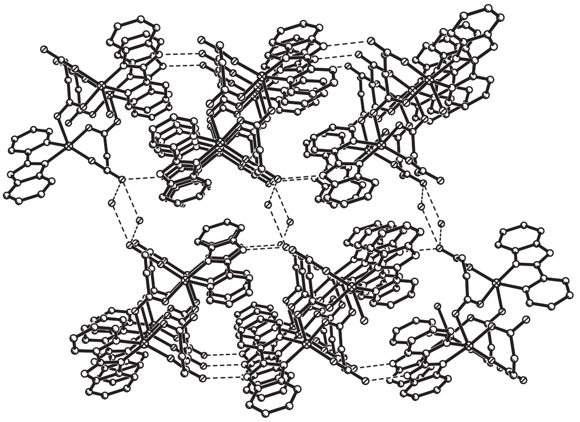

(d)

Figure 1. Continued.

pb ligands and the two bridging crotonates are almost perpendicular to each other with the dihedral angle range of 80.06–105.89°. The atoms in the axial O–Cu–Cu–O fragment are not collinear but considerably bent with O3A–Cu1–Cu2 and Cu1–Cu2–O5 angles of 155.14(2) and 162.85(2)°, respectively. Viewed from the whole compound, the four copper atoms arrange in a linear, quasi-zigzag configuration. Of particular interest in **2** is that the terminal MeOH, caps the copper atoms, inhibiting the complex from generating an infinite structure. Many monocarboxylates form oligo-nuclear compounds but not the unusual linear multi-nuclear structure. The formation of compound **2** may provide significant information for rational design of finite-chain supramolecular synthons. Another interesting point is that crotonate anions in complex **2** exhibit unusual μ_3-O monoatomic-bridging besides the familiar bidentate bridging. As a result, **2** has a Cu_2O_2 core with Cu1 ⋯ Cu1A separation of 3.455 Å and Cu1–O3–Cu1A angle of 104.86(3)°. The monoatomic O3 occupies simultaneously the apical site of Cu1A and the basal position of Cu1. The number of similar complexes with this Cu_2O_2 core (O derivative from aqua, hydroxo, carboxylato, alioxo, *etc.*) with two O atoms in equatorial–axial positions is rather limited. Recently, one complex

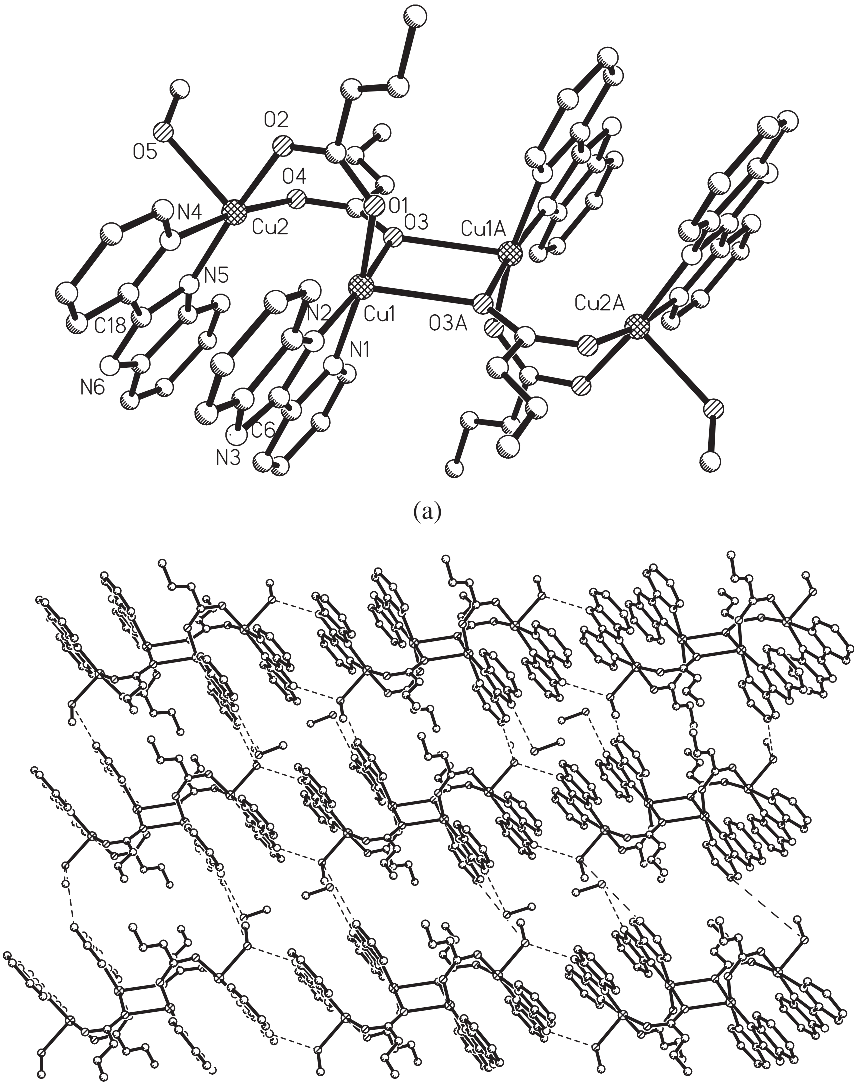

(a)

(b)

Figure 2. (a) The linear tetranuclear unit of **2**, hydrogen atoms and uncoordinated MeOH omitted for clarity. (b) The 2D network with MeOH located in the grids.

containing the same Cu_2O_2 core was reported by Chaudhuri *et al.* [18] as a polymer that cannot be broken into a finite structure. It is easier for complexes containing bridging ligands to form infinite polymers than finite structures. Hydrogen bonding interactions of N6 $\cdots$ H5A–O5 (2.373 Å, 169.36°) and C3–H3 $\cdots$ O5 (3.561 Å, 152.91°) between deprotonated pb and the capping MeOH can be observed, resulting in a 2D grid network together with π–π stacking interactions in which solvent MeOH are located in the grids by N $\cdots$ H–O hydrogen bonding (figure 2b).

On changing the crotonate to α-methacrylate in complex **2**, a dinuclear complex **3**, where two copper(II) ions in distorted square-pyramidal arrangement (figure 3a)

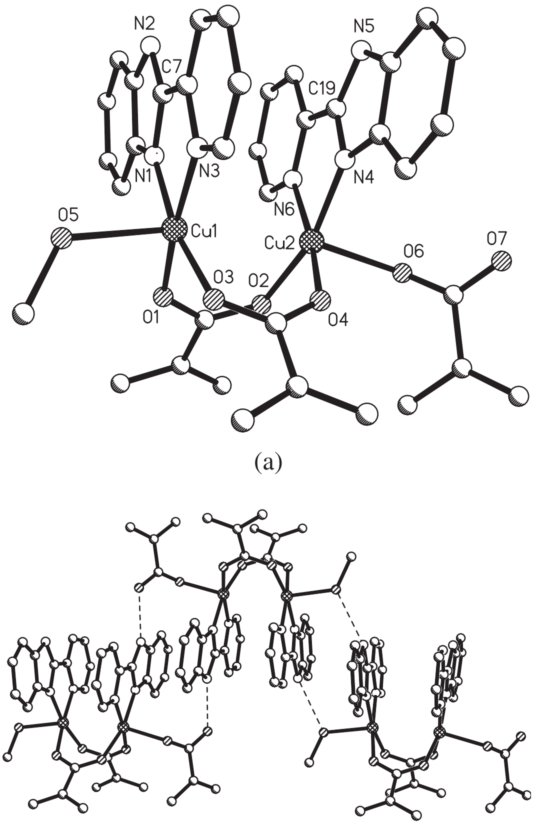

(a)

(b)

Figure 3. (a) The coordination environment of Cu ions in **3**, hydrogen atoms omitted for clarity. (b) The 1D sinusoidal chain formed by hydrogen bonding and π–π stacking interactions.

are separated by 3.055(3) Å, longer than the distance of the dimeric unit in **2** (2.989(3) Å). The deviations of Cu1 away from the basal planes of N1, N3, O1, O3 is 0.1527 Å towards O5, while Cu2 deviates 0.2050 Å away from the plane N4, N6, O2, O4 towards O6. Skeleton O–Cu–Cu–O bend slightly with O5–Cu1–Cu2 170.68° and Cu1–Cu2–O6 166.08° respectively, more than in **2**. The antiparallel Hpb and the two bridging α-methacrylates are almost perpendicular to each other with the dihedral angle range of 87.65–97.99°. In complex **3**; the basal plane α-methacrylate coordinates to copper(II) in bidentate bridging fashion but not exo-bridging to the next unit through a monoatomic bridge, different from **2**, owing to the steric hindrance of α-positioned methyl. In **3** the two antiparallel Hpb's are in different forms: the one close to MeOH is deprotonated while the one adjacent to α-methacrylate is neutral, obviously different from the four deprotonated Hpb coligands in complex **2** and also different from the all neutral ligand in **1**. In addition, Hpb as hydrogen bonding donors and acceptors provides O5–H5B$\cdots$N2 (2.819 Å, 176.83°) between O5 from MeOH and N2 from deprotonated pb and N5–H5A$\cdots$O7 (2.625Å, 166.80°) between N5 of neutral Hpb and O7 of uncoordinated carboxyl oxygen, which leads to a 1D sinusoidal structure (figure 3b) along with π–π stacking interactions.

When acrylate, an analogous carboxylate ligand of smaller size, takes the place of α-methacrylate, a mononuclear molecule is formed in **4** (figure 4a). It consists of a chelating Hpb ligand (average Cu–N 2.017(5) Å), two monodentate coordinated acrylate ligands (average Cu–O 1.954(5) Å) and a water molecule (Cu1–O5 2.248(4) Å) to furnish copper(II) a distorted square-pyramidal geometry. The deviation of Cu1 away from the equatorial plane (N1, N2, O1, O3) is 0.260 Å towards O5. Two acrylate ligands are almost perpendicular to the basal plane with the dihedral angle of 90.22 and 93.15°, respectively. In complex **4**, there exist four kinds of hydrogen bonding interactions with different functions for the formation of the supramolecule: (1) the intra-molecular hydrogen bonding O5–H5A $\cdots$ O4 (2.675 Å, 159.67°) being responsible for the overall stability of the complex; (2) the inter-molecular hydrogen bonding N3–H3A $\cdots$ O2 (2.774 Å, 161.55°) generating the dimeric unit, viz. supramolecular synthon; (3) the inter-dimer O5–H5B $\cdots$ O2 (2.808 Å, 120.37°) extending the synthon into a 1D ladder-shaped double chain (figure 4b) together with π–π stacking interactions of Hpb; (4) the inter-chain C2–H2 $\cdots$ O1 (3.354 Å, 133.42°) and C2–H2 $\cdots$ O4 (3.401 Å, 133.02°) resulting in an intriguing 3D columnar supramolecular network with open channels (figure 4c).

In **2**, **3** and **4**, the three α,β-unsaturated carboxylate copper(II) complexes have similar dinuclear cage conformation, but the topological structures of their Hpb complexes are different according to the variety of carboxylate coordination modes. In **2** and **3**, the carboxylate groups adopt familar bidentate bridging coordination and the structural motif $\{Cu_2(\mu\text{-}OCO)_2\}$ can be viewed as the result of the similar dimeric $Cu_2(CH_3CH{=}CHCO_2)_4(H_2O)_2$ and $Cu_2[CH_2{=}C(Me)CO_2]_4(H_2O)_2$ by replacing two out of the four carboxylate bridges by two Hpb ligands which sustain the dicopper moiety by π–π stacking interactions. In **2** crotonate adopts unusual μ_3-monoatomic-bridging besides bidentate bridging modes. As a result, four copper atoms are bridged by four crotonate anions and arranged in linear quasi-zigzag. The capping methanol molecules are responsible for inhibiting the finite chain from forming an infinite polymer. Complex **4** is a mononuclear molecule in which two monodentate acrylate anions coordinate to Cu, a classical dinuclear cage complex. On the other hand, coligands Hpb in the four complexes have different forms. From the crystallographic data it can be seen that Hpb are all deprotonated in **2** (N2–C6 1.354(4), N3–C6 1.325(4), N5–C18 1.360(3), N6–C18 1.330(4) Å), half deprotonated in **3** (N1–C7 1.349(8), N2–C7 1.336(8), N4–C19 1.334(8), N5–C19 1.357(10) Å), neutral in **1** (N2–C6 1.331(5), N3–C6 1.337(5) Å) and **4** (N2–C6 1.322(5), N3–C6 1.351(5) Å). When Hpb is neutral, the bond length of uncoordinated nitrogen and carbon from benzimidazole is longer than the length of coordinated nitrogen and carbon. Contrarily, when Hpb is deprotonated, the bond length of uncoordinated nitrogen and carbon is shorter than the length of coordinated nitrogen and carbon. The deprotonation mechanism of Hpb in different complexes is being studied.

3.2. *Thermogravimetric analysis*

The thermogravimetric analysis (TGA) curve of **1** exhibits three continuous weight loss stages in the temperature ranges 25–150, 200–300 and 320–550°C, corresponding to the concomitant release of uncoordinated water, maleate and Hpb. The residue is CuO. The whole weight loss (80.11%) is in good agreement with the calculated value (79.54%). Thermogravimetric analysis indicates that compound **2** has good stability.

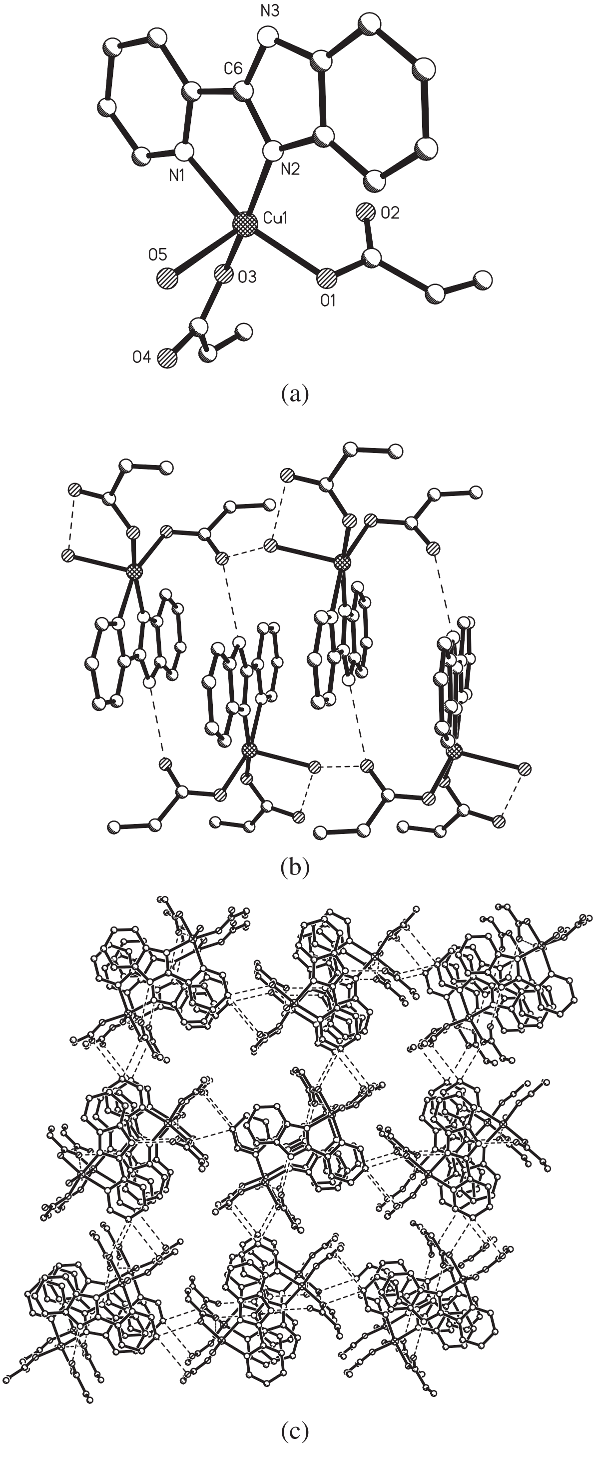

Figure 4. (a) The coordination environment of Cu^{2+} in **4**, hydrogen atoms omitted for clarity. (b) The 1D ladder-shaped double chain. (c) The 3D supramolecular network extended by the 1D ladder-shaped double chain through C–H $\cdots$ O hydrogen bonding.

The TGA curve exhibits no weight loss from room temperature to 150°C. The weight loss occurs at the temperature range 170–295°C and 305–600°C, corresponding to the release of methanol, crotonate and Hpb with total weight loss of 79.23%. The residue is also CuO. For complex **3**, the most significant weight loss occurs in the range 80–310°C, suggesting the loss of methanol, methacrylate anions and Hpb. The residue of 19.85% is consistent with the final CuO, close to the expected values of 19.46%. For complex **4**, the first weight loss corresponds to a coordinated water molecule in the range 60–150°C. The second weight loss in the range 180–550°C is close to the loss of acrylate anions and Hpb. The residue of 20.55% above 600°C corresponds to the expected CuO values (20.47%).

3.3. *Magenetic properties*

The temperature dependence of the χ_M and μ_{eff} curves for complexes **1**, **2** and **3** are shown in figure 5. For complex **1** χ_M increases in a uniform way from 0.0012 $cm^3\,mol^{-1}$ at 300 K to 0.088 $cm^3\,mol^{-1}$ at 7 K (figure 5a). The μ_{eff} value at room temperature, 1.72 μ_B, is close to the spin-only value for Cu^{II} (1.73 μ_B). Starting from 300 K the μ_{eff} value smoothly increases up to 47 K and below 22 K increases quickly. The shape of this μ_{eff} curve is indicative of weak ferromagnetic coupling.

The magnetic behavior of **1** has been analyzed with a theoretical expression from the Bonner-Fisher model [19]. The best fit of the experimental data lead to $J = 1.95\,cm^{-1}$, $g = 1.98$ and $R = 5.78 \times 10^{-5}$, where $R = \sum[(\chi_M T)_{exp} - (\chi_M T)_{calc}]^2 / \sum[(\chi_M T)_{exp}]^2$. These results indicate a weak ferromagnetic interaction between Cu^{II} centers due to the syn–anti carboxylate bridging mode and are in good agreement with the experimental results.

The magentic behavior of **2** is shown in figure 5(b). The χ_M curve starts at 0.0058 $cm^3\,mol^{-1}$ at 300 K and increases in a uniform way to the maximum of 0.0195 $cm^3\,mol^{-1}$ at 50 K, then decreases to the minimum of 0.0002 $cm^3\,mol^{-1}$ at 9 K. Below 9 K a paramagnetic tail appears, arising from the contributions of the presence of a small amount of impurities in the power sample, exhibiting paramagnetism. The maximum at low temperature indicates a weak antiferromagnetic coupling between Cu^{II} centers. The value of μ_{eff} at 300 K is 3.74 μ_B, which is as expected for four magnetically quasi-isolated spin doublets. The μ_{eff} value smoothly decreases down to 90 K and then quickly decreases to 9 K. The global feature is characteristic of weak antiferromagnetic interaction.

As shown in the crystallographic section, in **2** the bridging oxygen atoms from the Cu_2O_2 core belong to the equatorial plane of one Cu^{II} center but to the apical position of the neighbouring Cu^{II} center. For the first Cu^{II} center, the oxygen atom is well directed to the magnetic orbital ($dx^2 - y^2$) but not properly directed to the other Cu^{II} center (dz^2). This geometry avoids any important overlap between both copper atoms, resulting in very small (but not negligible) coupling. Based on the above considerations, it can be considered that only one important interaction exists, J_1 within dimers, assuming an ideal Cu_2 entity using the Bleaney-Bowers formula [20, 21] and calculating the possible J_2 (from Cu_2O_2 core) using the molecular-field approximation [21]. It gives the best final parameters: J_1 (Cu2–Cu1) $= -26.9\,cm^{-1}$, J_2 (Cu1–Cu1A) $= 7.69\,cm^{-1}$, $g = 2.00$, and $R = 3.46 \times 10^{-4}$. These J values indicate that the intra-dimeric syn–syn carboxylate bridges create medium antiferromagnetic coupling, as expected, whereas the inter-dimeric monoatomic bridges create small

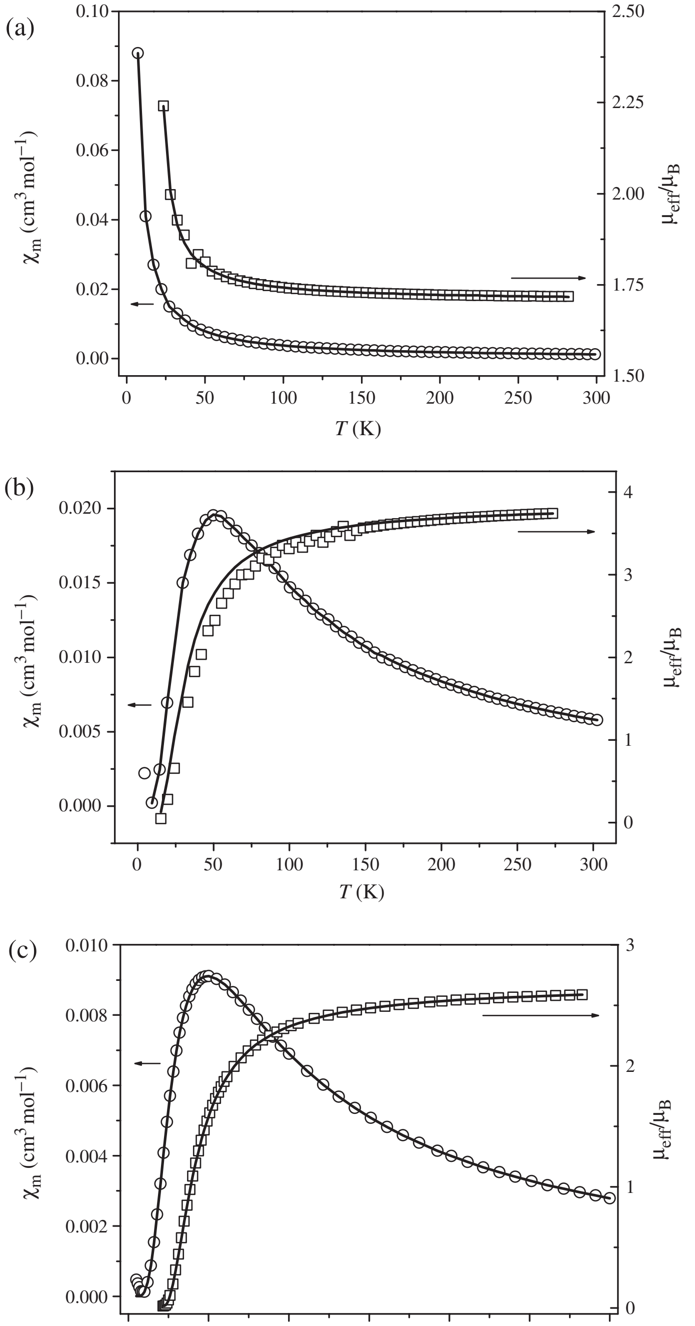

Figure 5. (a) The magnetization curve of complex **1**. (b) The magnetization curve of complex **2**. (c) The magnetization curve of complex **3**.

ferromagnetic coupling consistent with the fact [18] of a very small but not negligible coupling in complexes with Cu_2O_2 core in equatorial–axial positions.

The magnetic property of **3** is very similar to **2** (figure 5c), revealing strong antiferromagentic coupling between pairs of Cu^{II} centers. Below 10 K a paramagnetic tail appears also, exhibiting some monomer impurities in the complex. The value of μ_{eff} at 300 K is 2.58 μ_B. This value corresponds to two uncoupled Cu^{II} ions with $g > 2.00$. The magnetic susceptibilities per Cu ion may be calculated using the expression from the Bonner-Fisher calculation [22]. The best-fit parameters are found as $J = -55.27$, $g = 2.17$ and $R = 5.57 \times 10^{-9}$. The strong antiferromagnetic coupling in the dimer is in the value range [18] of two syn–syn carboxylate bridges in dinuclear copper(II) complexes.

The magnetic behaviours of complex **1**, **2** and **3** show that for copper(II) complexes, syn–anti μ-OCO bridging mode presents weak ferromagnetic coupling, syn–syn μ-OCO conformation mediates a large to antiferromagnetic coupling and monoatomic μ-O bridging fashion of –COO group is predominantly slightly ferromagnetic.

4. Conclusions

Similar α,β-unsaturated carboxylate copper(II) and coligand Hpb, have resulted in four unique supramolecular entities with different structures. We have demonstrated that the different coordination adopted by different carboxylate anions result in different complexes and different magnetic behavior. The coligand Hpb (deprotonated and/or neutral) provides hydrogen bonding and π–π stacking interactions responsible for the formation of supramolecular frameworks. Complex **2** is an unusual finite-chain complex based on monocarboxylate. Variable-temperature magnetic behavior of complexes **1**, **2** and **3** indicate that for copper(II) complexes, syn–anti bridging gives weak ferromagenetic coupling, syn–syn conformation mediates large antiferromagnetic coupling and monoatomic bridging presents weak ferromagentic coupling.

Supplementary material

X-ray crystallographic files in CIF format have been deposited with the Cambridge Structural Detabase as files CCDC 261527, 261526, 271334 and 271333 for crystals **1**, **2**, **3** and **4**. This material is available free of charge *via* the Internet at http://pubs.acs.org.

Acknowledgements

We thank the financial support from the National Natural Science Foundation of China (No. 20471048) and TRAPOYT.

References

[1] (a) J.W. Steed, J.L. Atwood. *Supramolecular Chemistry*, Wiley and Sons, New York (2000). (b) J.M. Lehn. *Supramolecular Chemistry: Concepts and Perspectives*, VCH, New York (1995).

[2] (a) S.R. Batten, R. Robson. *Angew. Chem. Int. Ed.*, **37**, 1460 (1998). (b) S. Leininger, B. Olenyuk, P.J. Stang. *Chem. Rev.*, **100**, 853 (2000). (c) G.F. Swiegers, T.J. Malefetse. *Chem. Rev.*, **100**, 3483 (2000).

(d) B. Moulton, M.J. Zaworoko. *Chem. Rev.*, **101**, 1629 (2001). (e) D.L. Caulder, K.N. Raymond. *Acc. Chem. Res.*, **32**, 975 (1999).

[3] (a) B.J. Holliday, C.A. Mirkin. *Angew. Chem. Int. Ed.*, **40**, 2023 (2001). (b) T. Caronna, R. Liantonio, T.A. Logothetis, P. Metrangolo, T. Pilati, G. Resnati. *J. Am. Chem. Soc.*, **126**, 4500 (2004). (c) D.F. Sun, R. Cao, Y.Q. Sun, W.H. Bi, X.J. Li, Y.Q. Wang, Q. Shi, X. Li. *Inorg. Chem.*, **42**, 7512 (2003).

[4] (a) R. Sang, L. Xu. *Inorg. Chem.*, **44**, 3731 (2005). (b) D.K. Cao, Y.Z. Li, Y. Song, L.M. Zheng. *Inorg. Chem.*, **44**, 3599 (2005).

[5] (a) K.T. Holman, A.M. Pivovar, J.A. Swift, M.D. Ward. *Acc. Chem. Res.*, **34**, 107 (2001). (b) K. Biradha. *Cryst. Eng. Comm.*, **5**, 274 (2003).

[6] (a) Y.G. Li, N. Hao, E.B. Wang, Y. Lu, C.W. Hu, L. Xu. *Eur. J. Inorg. Chem.*, **14**, 2567 (2003). (b) W. Lu, N.Y. Zhu, C.M. Che. *J. Am. Chem. Soc.*, **125**, 16081 (2003). (c) M. Eddaoudi, J. Kim, N. Rosi, D. Vodak, J. Wachter, M. O'Kee, O.M. Yaghi. *Nature*, **295**, 469 (2002). (d) A. Chaudhuri, S. Natarajan, C.N.R. Rao. *Chem. Mater.*, **11**, 2316 (1999).

[7] D. Ghoshal, T.K. Maji, G. Mostafa, T.H. Lu, N.R. Chaudhuri. *Cryst. Growth. Des.*, **3**, 9 (2003).

[8] (a) K.M. Buschbaum, C.C. Quitmann. *Inorg. Chem.*, **42**, 2742 (2003). (b) D. Choquesillo-Lazarte, B. Covelo, J.M. González-Pérez, A. Castiñeiras, J. Niclós-Gutiérrez. *Polyhedron*, **21**, 1485 (2002).

[9] (a) B.H. Ye, M.L. Tong, X.M. Chen. *Coord. Chem. Rev.*, **249**, 545 (2005). (b) O.R. Evans, W.B. Lin. *Acc. Chem. Res.*, **35**, 511 (2002).

[10] S. Konar, P.S. Mukherjee, F. Lloret, E. Zangrando, N.R. Chaudhuri. *Angew. Chem., Int. Ed.*, **41**, 1561 (2002).

[11] (a) A.M. Madalan, C. Paraschiv, J.P. Sutter, M. Schmidtmann, A. Müller, M. Andruh, *Cryst. Growth. Des.*, **5**, 707 (2005). (b) L.Y. Zhang, G.F. Liu, S.L. Zheng, B.H. Ye, X.M. Zhang, X.M. Chen. *Eur. J. Inorg. Chem.*, **16**, 2965 (2003).

[12] (a) H.R. Ma, Y.Y. Wang, P. Liu, D.S. Li, Q.Z. Shi, G.H. Lee, S.M. Peng. *Polyhedron*, **24**, 215 (2005). (b) X.J. Luan, Y.Y. Wang, D.S. Li, P. Liu, H.M. Hu, Q.Z. Shi, S.M. Peng. *Angew. Chem. Int. Ed.*, **44**, 3864 (2005). (c) D.S. Li, Y.Y. Wang, X.J. Luan, P. Liu, C.H. Zhou, H.R. Ma, Q.Z. Shi. *Eur. J. Inorg. Chem.*, **13**, 2678 (2005).

[13] Y.Y. Wang, Q. Shi, Q.Z. Shi, Y.C. Gao, Z.Y. Zhou. *Polyhedron*, **18**, 2009 (1999).

[14] G.M. Sheldrick. *SHELXS 97, Program for Crystal Structure Solution*, University of Göttingen, Germany (1997).

[15] G.M. Sheldrick. *SHELXS 97, Program for Crystal Structure Refinement*, University of Göttingen, Germany (1997).

[16] M.H. Molina, C.R. Pérez, T. López, F. Lloret, M. Julve. *Inorg. Chem.*, **42**, 5456 (2003).

[17] S.G. Ang, B.W. Sun. *Cryst. Growth. Des.*, **5**, 383 (2005).

[18] D. Ghoshal, T.K. Maji, G. Mostafa, S. Sain, T.H. Lu, J. Ribas, E. Zangrando, N.R. Chaudhuri. *J. Chem. Soc., Dalton Trans.*, **11**, 1687 (2004).

[19] M.E. Fisher. *Am. J. Phys.*, **32**, 343 (1964).

[20] B. Bleaney, K.D. Bowers. *Proc. R. Soc. London, Ser. A.*, **214**, 45 (1952).

[21] O. Kahn. *Molecular Magnetism*, VCH, New York (1993).

[22] M. Kato. *Coord. Chem. Rev.*, **92**, 45 (1988).